

A Nonlinear State Observer for the Bi-Hormonal Intraperitoneal Artificial Pancreas

Karim Davari Benam^{a,1}, Hasti Khoshamadi^{a,2}, Laura Lema-Pérez^{a,3},
Sebastien Gros^{a,4}, Anders Lyngvi Fougner^{a,5}

Abstract—Currently, continuous glucose monitoring sensors are used in the artificial pancreas to monitor blood glucose levels. However, insulin and glucagon concentrations in different parts of the body cannot be measured in real-time, and determining body glucagon sensitivity is not feasible. Estimating these states provides more information about the current system status, facilitating improved decision-making by the model-based controller. In this regard, the aim of this paper is to design a nonlinear high-gain observer for a bi-hormonal artificial pancreas in the presence of measurement noises, model uncertainties, and disturbances. The model used in the observer is based on an existing intraperitoneal nonlinear animal model in the literature. This model is modified by assuming that insulin can directly transfer from the peritoneal cavity to the bloodstream. Based on a set of realistic assumptions, one model is considered after each hormone infusion, and two observers are separately designed. The model is divided into the insulin-phase and glucagon-phase models based on a set of realistic assumptions. Thereafter, two high-gain observers are designed separately for these phases contributing to estimating the non-measurable states. The observer error is proven to be locally uniformly ultimately bounded, and it is verified that any asymptotically stable control laws remain stable in the presence of the observer. The performance of the observers with different gains is evaluated for a scenario with multiple insulin and glucagon infusions. The proposed observer converges to a finite error, according to the results.

Clinical relevance— In Type 1 diabetic patients, the developed observer can be employed in a closed-loop artificial pancreas to improve the performance of model-based controllers. It estimates the key states, which are necessary for forecasting the body's response to insulin and glucagon boluses.

I. INTRODUCTION

Glucose homeostasis is a mechanism of critical importance for sustaining life in humans through the use of glucose as a source of energy. One of the main organs involved in this mechanism is the pancreas. The pancreas regulates glucose in the body autonomously and continuously. The glycemic control is primarily achieved through the pancreas' endocrine hormones balanced through a negative feedback loop. Insulin and glucagon are the essential pancreatic hormones that affect the blood glucose level (BGL). Insulin (produced by beta cells in the pancreas) decreases BGL by either storing

excess glucose mainly in the liver and muscles or allowing body cells to utilize glucose as fuel. Glucagon (produced by pancreatic alpha cells) raises BGL by releasing glucose that has been stored as glycogen in the body.

Type 1 diabetes (T1D), or insulin-dependent diabetes, is a chronic disease where the pancreas produces no or little insulin. T1D has an unknown etiology. In most cases, T1D is caused by a reaction of the immune system destroying the beta cells of the pancreas. Other possible explanations include genetics, viral exposure, and other environmental variables. Impaired glucagon production and release are also common as a consequence of beta cells destruction. Therefore, the body becomes incapable of maintaining a normal BGL [1], [2].

An artificial pancreas (AP) that consists of subcutaneous BGL sensor(s), insulin/ and glucagon pump(s), and a control algorithm is the current treatment for T1D disease. It mimics the natural endocrine pancreas function by automatically delivering external insulin and glucagon in response to the changes in BGL. Different versions of single-hormone APs that infuse only insulin are currently available on the market [3]. However, since these systems lack glucagon, there is a substantial risk of low BGL if unannounced physical activities are performed. Dual-hormone APs are under development and the prior clinical trials show their advantages in reducing the number of hypoglycemia episodes [4].

It is possible to deliver hormones intravenously (IV), subcutaneously (SC), and intraperitoneally (IP). Although the IV route is fast, it is not a practical continuous solution due to the possible health complications. SC infusion is the most common approach in delivering insulin in current APs. However, due to the SC route's absorption delay, the existing APs, even with the most advanced control algorithms, are ineffective in dealing with unannounced meals [5].

The IP drug delivery pathway has been shown to have faster pharmacokinetics than the SC pathway [3]. Furthermore, in IP insulin infusion, the majority of the insulin absorbs into the portal vein (PV) and is then delivered to the liver. While in SC infusion, insulin first absorbs into the blood circulation system before reaching the liver. As a result, the IP insulin infusion seems to be physiologically more similar to pancreatic functionality. Moreover, Toffanin *et al.* tested their AP with IP infusion on the modified UVA/Padova simulator [6] and showed that the meal announcement is not needed [5].

Model-based controllers, such as model predictive control (MPC), are the most commonly used control approaches in

*This research is funded by the Research Council of Norway (project no. 248872), and the Centre for Digital Life Norway.

^a Department of Engineering Cybernetics, Faculty of Information Technology and Electrical Engineering, Norwegian University of Science and Technology (NTNU), O. S. Bragstads Plass 2D, 7034 Trondheim, Norway.

¹ karim.d.benam@ntnu.no

² hasti.khoshamadi@ntnu.no

³ laura.l.perez@ntnu.no

⁴ sebastien.gros@ntnu.no

⁵ anders.fougner@ntnu.no

APs due to the constraints and the delays [7]. However, BGL is the only real-time measurable output of the system, while the other states essential for prediction must be estimated. In this paper, a high-gain observer is developed to estimate non-measurable states based on a modified version of the nonlinear bi-hormonal-glucose model proposed in [8]. High-gain observer is chosen due to its implementation simplicity and its robustness against large perturbations and model uncertainties. In spite of measurement noise, model mismatches, and disturbances, the proposed observer is proven to converge to a bounded error under some assumptions. Furthermore, the Lyapunov theorem is used to demonstrate that any asymptotically stable control approach will remain stable when the designed observer is used in the control loop.

The paper is organized as follows: In Section II, the modified version of the nonlinear bi-hormonal-glucose model is introduced and practical assumptions for designing the observer are made. Section III presents the high-gain observers designed for the insulin and glucagon phases and the convergence analysis. Results are discussed in Section IV. Finally, conclusions are exposed in Section VI.

II. MATHEMATICAL MODEL AND ASSUMPTIONS

The nonlinear bi-hormonal-glucose model developed by Zazueta *et al.* [8] describes the interaction of BGL with IP insulin and glucagon, making it appropriate for bi-hormonal APs. In order to ensure structural identifiability, the effect of the insulin in the intermediate compartment is ignored and the order of the model is reduced in their final model.

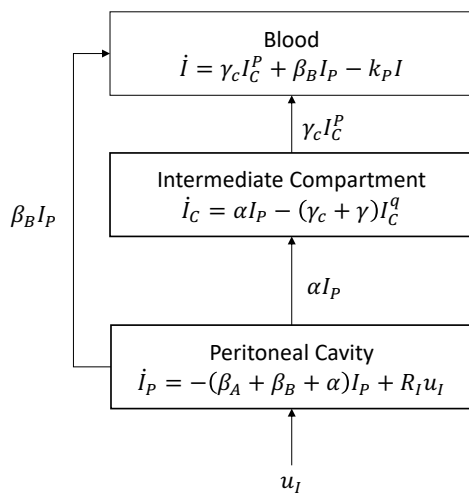


Fig. 1. Block diagram of the insulin compartment.

A modified version of this model is used to construct the observer in this paper. This modified version is as follows

$$\dot{G} = -[k_1 + k_I I + k_{I_c} I_c] G + k_H H f(\xi) + R \quad (1)$$

$$\dot{I} = \gamma_c I_c^p + \beta_B I_p - k_p I \quad (2)$$

$$\dot{I}_c = \alpha I_p - (\gamma_c + \gamma) I_c^q \quad (3)$$

$$\dot{I}_p = -(\beta_A + \beta_B + \alpha) I_p + R_I u_I(t) \quad (4)$$

$$\dot{H} = -n H + n_2 h_1 \quad (5)$$

$$\dot{h}_1 = -n_1 h_1 + R_H u_H(t) \quad (6)$$

$$\dot{\xi} = x_1 [(k_I I + k_{I_c} I_c) G] - x_2 [H f(\xi)] - x_3 \xi \quad (7)$$

where $f(\xi) = \xi^a$ for $0 < a \leq 1$ (where $a = 1$ in the original model). As it is shown in Fig. 1, the pathway of direct insulin transportation from the peritoneal cavity to the blood is considered in this model as described in [9]. In addition, $-x_3 \xi$ is added in (7) to model the glucagon sensitivity decrease due to the basal endogenous glucagon production. The states, inputs, and parameters of the model are described in Table I.

TABLE I
STATES, PARAMETERS, AND INPUTS OF THE MODEL.

Symbol	Description	Unit
States		
G	Blood glucose concentration.	mmol/L
I	Blood insulin concentration.	mU/L
I_c	Insulin concentration in the intermediate compartment.	mU/L
I_p	Insulin concentration in peritoneal cavity.	mU/L
H	Blood glucagon concentration.	pmol/L
h_1	Glucagon concentration in peritoneal cavity.	pmol/L
ξ	Glucagon sensitivity.	dimensionless
Inputs		
R	IV exogenous glucose infusion.	mmol/L/h
u_I	IP insulin bolus.	U
u_H	IP glucagon bolus.	μg
Parameters		
k_1	Insulin-independent removal rate of glucose.	1/h
k_I, k_{I_c}	Insulin-dependent removal rates of glucose.	L/mU/h
k_H	Glucose response to glucagon rate.	1/h
k_p, γ, β_A, n	Consumption and degradation rates.	1/h
$\gamma_c, \alpha, \beta_B, n_1, n_2$	Transport rates.	1/h
a, p, q	Powers.	dimensionless
R_I	Conversion parameter.	1/L/h
R_H	Conversion parameter.	pmol/ μg /L/h
x_1	Conversion parameter.	L/mmol
x_2	Conversion parameter.	L/pmol/h
x_3	Decrease rate of glucagon sensitivity due to endogenous glucagon production.	1/h

As mentioned in the introduction, a state observer is needed to estimate the non-measurable states for a model-based controller, such as an MPC, to make better control decisions. To design a high-gain observer, the following assumptions are considered:

- 1) The amounts of insulin and glucagon in the peritoneal cavity are represented by I_p and h_1 . The inputs and parameters used in (4) and (6) are assumed to be known. Therefore these states can be calculated, and there is no need for the observer to estimate them.

- 2) Insulin and glucagon are hormones with reverse effects on BGL. It is not typical to design controllers in AP to use these hormones simultaneously or close to each other. Therefore, an observer during each of these hormone infusions can be designed separately.
- 3) For simplicity, it is assumed that $p = 1$ and $q = 1$.

Two different models are considered, one during the insulin phase and the other during the glucagon phase, in order to design the observers:

• Insulin-phase Model

$$\dot{G}_I = -[k_1 + k_I I + k_c I_c] G_I + k_H \hat{H} f(\hat{\xi}) + R \quad (8)$$

$$\dot{I} = \gamma_c I_c + \beta_B I_p - k_p I \quad (9)$$

$$\dot{I}_c = \alpha I_p - \gamma_c I_c - \gamma I_c \quad (10)$$

$$y_m = G_I + v \quad (11)$$

where G_I is blood glucose concentration during the insulin phase, v is the measurement noise, and y_m is the measured BGL. Moreover, \hat{H} and $\hat{\xi}$ are the estimated states from the glucagon phase.

• Glucagon-phase Model

$$\dot{G}_H = -[k_1 + k_I \hat{I} + k_{I_c} \hat{I}_c] G_H + k_H H f(\xi) + R \quad (12)$$

$$\dot{\xi} = x_1 \left[(k_I \hat{I} + k_{I_c} \hat{I}_c) G \right] - x_2 [H f(\xi)] - x_3 f(\xi(t)) \quad (13)$$

$$\dot{H} = -nH + n_2 h_1 \quad (14)$$

$$y_m = G_H + v \quad (15)$$

where G_H is blood glucose concentration during the glucagon phase. \hat{I} and \hat{I}_c are estimations from the insulin phase.

It is worth mentioning that each of these models is observable. In the next section, a high-gain observer is designed, and its convergence and error bounds are analyzed.

III. HIGH-GAIN OBSERVER AND CONVERGENCE ANALYSIS

The high-gain observer is one of the most commonly used nonlinear observers that considers both measurement noises and model uncertainties [10]. In this section, two high-gain observers are proposed for insulin phase and glucagon phase models.

A. Nominal Form of Models

To simplify the stability analysis and take advantage of the high-gain observer, each model must be transformed into a nominal form [11]. For this purpose, the new states for the insulin-phase and glucagon-phase models are defined as

$$S_1 \stackrel{\text{def}}{=} [p_1 \quad q_1 \quad r_1]^T \quad (16)$$

$$S_2 \stackrel{\text{def}}{=} [p_2 \quad q_2 \quad r_2]^T \quad (17)$$

where $[p_1, q_1, r_1]^T$ and $[p_2, q_2, r_2]^T$ are defined in (18) and (19), respectively. In these two equations, $e_1 \triangleq k_I k_p$, $e_2 \triangleq$

$-k_I \gamma_c - k_c (\gamma_c + \gamma)$, $e_3 \triangleq k_c a + k_I \beta_B$, $e_4 \triangleq (k_1 + k_I \hat{I} + k_{I_c} \hat{I}_c)$, and $e_5 = k_H f(\xi)$.

The state-space models are transformed into the following equations for $i=1,2$:

$$\dot{S}_i = A S_i + B \varphi_i(S_i, u_i, R) \quad (20)$$

$$y_m = C S_i + v \quad (21)$$

where $\varphi_i(S_i, u_i, R) \triangleq r_i$, $u_1 \triangleq I_p$, $u_2 \triangleq h_1$,

$$A = \begin{bmatrix} 0 & 1 & 0 \\ 0 & 0 & 1 \\ 0 & 0 & 0 \end{bmatrix}, \quad B = \begin{bmatrix} 0 \\ 0 \\ 1 \end{bmatrix}$$

, and $C = [1 \quad 0 \quad 0]$. Furthermore, $\|v\| < \mu$ for positive values of μ as the maximum amplitude of measurement noise.

B. High-Gain Observer

A high-gain observer is designed based on the formulation proposed in [11], [12] as follows

$$\dot{\hat{S}}_i = A \hat{S}_i + B \varphi_{o_i}(\hat{S}_i, u_i, R) + \frac{1}{\varepsilon_i} H_i (y_m - C \hat{S}_i) \quad (22)$$

where \hat{S}_i for $i = \{1, 2\}$ is the estimation of S_i , ε_i is the inverse of observer gain, and φ_{o_i} is the nominal form of φ_i . It is notable that φ_i is locally Lipschitz function of S_i and u_i . In addition, for arbitrary positive values of $\{a_{i1}, a_{i2}, a_{i3}\}$, H_i is defined as follows

$$H_i = \begin{bmatrix} \frac{a_{1i}}{\varepsilon_i} & \frac{a_{2i}}{\varepsilon_i^2} & \frac{a_{3i}}{\varepsilon_i^3} \end{bmatrix}^T \quad (23)$$

Moreover, the weighted observer error for $\varepsilon_i \in (0, 1)$ is defined as

$$\eta_i = D(\varepsilon_i)_{3 \times 3} (S_i - \hat{S}_i) \quad (24)$$

with

$$D(\varepsilon_i) \triangleq \begin{bmatrix} 1 & 0 & 0 \\ 0 & \varepsilon_i & 0 \\ 0 & 0 & \varepsilon_i^2 \end{bmatrix} \quad (25)$$

In the rest of the paper, since both models are in the nominal form, the index i is removed to increase readability.

Using (20) and (24), the dynamics of the system and the weighted observer error can be augmented as below.

$$\dot{S} = f_s(S, S - D(\varepsilon)^{-1} \eta, R) \quad (26)$$

$$\varepsilon \dot{\eta} = A_0 \eta + \varepsilon^2 B g(S, S - D(\varepsilon)^{-1} \eta, R) + B_2 v \quad (27)$$

where f_s is the right-hand side of the (20) with assuming that u_i is function of observed states. Moreover,

$$A_0 = \begin{bmatrix} -a_{i1} & 1 & 0 \\ -a_{i2} & 0 & 1 \\ -a_{i3} & 0 & 0 \end{bmatrix}, \quad B_2 = \begin{bmatrix} -a_{i1} \\ -a_{i2} \\ -a_{i3} \end{bmatrix}$$

, and $g(\dots) = \varphi(\dots) - \varphi_o(\dots)$. In addition, $\{a_{i1}, a_{i2}, a_{i3}\}$ should be selected in a way that eigenvalues of A_0 lay at left-half plane.

$$\begin{bmatrix} p_1 \\ q_1 \\ r_1 \end{bmatrix} \stackrel{\text{def}}{=} \begin{bmatrix} G_I \\ -(k_1 + k_I I + k_c I_c) G_I \\ -(k_1 + k_I t I + k_c I_c)^2 G_I - (e_1 I + e_2 I_c + e_3 I_p) \end{bmatrix} \quad (18)$$

$$\begin{bmatrix} p_2 \\ q_2 \\ r_2 \end{bmatrix} \stackrel{\text{def}}{=} \begin{bmatrix} G_H \\ -\left(k_1 + k_I \hat{I} + k_{I_c} \hat{I}_c\right) G_H + k_H H f(\xi) \\ -e_4 \dot{G}_H + a e_5^{\frac{a-1}{a}} H (x_1 e_4 G_H - (x_2 H + x_2) e_5) + e_5 (nH - n_2 h_1) + e_4 G \end{bmatrix} \quad (19)$$

Based on the *Lemma 1* in [11], the observer error (27) converges to a bounded set for

$$\|g(S, D(\varepsilon)^{-1}\eta, R)\| < k_g. \quad (28)$$

proof: Since A_0 is a Hurwitz matrix by design, a positive symmetric matrix E can be found such that $EA_0 + A_0^T E = -I$. Considering $W(\eta) = \eta^T E \eta$ as a Lyapunov candidate function, its time derivation is

$$\dot{W} \leq -\frac{1}{\varepsilon} \|\eta\|^2 + 2\varepsilon \|\eta\| \|EB\| k_g + \frac{2}{\varepsilon} \|\eta\| \|EB_2\| \mu. \quad (29)$$

It can be shown that

$$\Sigma = \left\{ W(\eta(t)) \leq \|E\| \left(4\|EB\| k_g \varepsilon^2 + 4\|EB_2\| \mu \right)^2 \right\} \quad (30)$$

is an invariant since $\dot{W}(\eta(t)) < -2/\varepsilon \|E\|$ for $W(\eta) \notin \Sigma$.

While $\|\eta\| \leq c_1 \varepsilon^2 + c_2 \mu$ for $W(\eta) \in \Sigma$, where $c_1 \triangleq 4\|EB\| k_g \sqrt{\|E\|/\sqrt{\lambda_{\min}(E)}}$ and $c_2 \triangleq 4\|EB_2\| \sqrt{\|E\|/\sqrt{\lambda_{\min}(E)}}$. Therefore, the designed observer converges to a bounded error which can be found by

$$\|S(t) - \hat{S}(t)\| \leq c_1 \varepsilon + c_2 \frac{\mu}{\varepsilon} \triangleq F_r(\varepsilon, \mu) \quad (31)$$

C. Stability of Closed-loop System in Presence of the Designed Observer

In this section, the stability of the closed-loop system in presence of the designed observer is analyzed as in [12].

We assumed that the closed-loop system is asymptotically stable for $S \in \Omega$ when $\eta = 0$. Therefore, there is a Lyapunov function $V(S) > 0$ (and $V(S) = 0$ for $S = 0$) in which $\dot{V}(S) < -U(S)$. Where $U(S)$ is positive function for $S \in \Omega$. Since $f(S, S - D(\varepsilon)^{-1}\eta)$ is bounded function and locally satisfies the Lipchitz conditions, one can write

$$\|f(S, D(\varepsilon)^{-1}\eta) - f(S, 0)\| \leq L_1 \|D(\varepsilon)^{-1}\eta\| \quad (32)$$

where L_1 is positive constant. In addition, one can assume $\|dV/dS\| \leq L_2$ for a positive value of L_2 . Using this inequalities, for $\eta \neq 0$, one can write

$$\dot{V}(S) \leq -U(S) + L_1 L_2 F_r(\varepsilon, \mu) \quad (33)$$

As it proven in [12], for bounded values of μ there is set of positive values for ε in which $F_r(\varepsilon, \mu) < U(S)/L_1 L_2$. That means the closed-loop system remains stable and $(S(t), \eta(t))$ will remain in $\{\Omega \times \Sigma\}$.

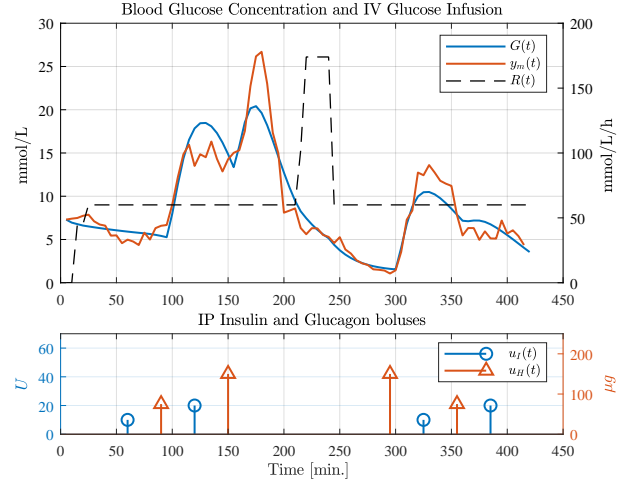


Fig. 2. The scenario used for evaluating the observer performance.

IV. RESULTS

In the development of an AP, there are non-measurable states that must be estimated so that the controller can make better decisions in the control of BGL regarding the treatment of people with T1D. The high-gain observer was designed based on the modified nonlinear bi-homonal-glucose model, and its convergence to a bounded error was evaluated.

To test the effectiveness of the observer, the scenario shown in Fig. 2 was considered where the sampling rate was set to 5 minutes, and four insulin boluses $\{10, 20, 10, 20\}U$, four glucagon boluses $\{75, 150, 150, 75\}\mu g$, and $R(t)$ as IV glucose infusion were given. Furthermore, the measured BGL ($y_m(t)$) was created by adding a measurement noise with the maximum amplitude of 2 mmol/L and a sinusoidal disturbance with amplitude 20% of the BGL and a frequency of 0.4 rad/h in order to evaluate the observer's robustness. Notably, 15% parameter identification error was considered to simulate the model uncertainties.

In order to analyze the error bound and time response of the observer, two cases are considered. In each case, there are two observers with the gain of ε_1 and ε_2 , respectively, for the insulin and glucagon phases. In the first case, relatively high values (near to one) were chosen both for ε_1 and ε_2 while these values were relatively low in the second case. The initial values were chosen randomly but the same for all observers in both cases.

In Fig. 3 and Fig. 4, the estimation results of the case 1 and

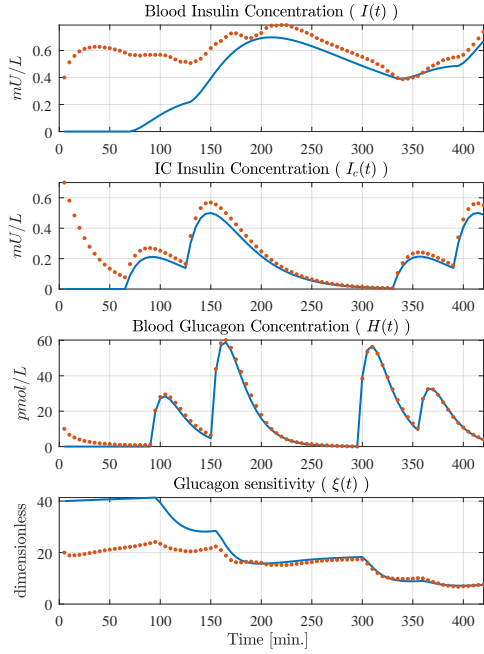


Fig. 3. Case 1: Performance of the designed observer with $\varepsilon_1 = 0.9$ and $\varepsilon_2 = 0.9$. The constant blue lines in this figure show the values of the states derived from the model, while the red dots are the outputs of the observers.

2 are shown, respectively. As can be seen, the estimations of the states using the designed observers converged to actual values with a bounded error. It can be noted that the performance of the designed observers with the lower gains (case 2) were faster while error boundaries increased.

As can be deduced from Fig. 3 and Fig. 4, there is a trade-off in selecting the observer gain, ε . The switching-gain observer concept described in [11] was used to address this issue. Based on this concept, it is better to initially have a small observer gain since it allows the observer to converge faster. Then, the observer gain can take a larger value T_s min after $\|y_m - \hat{y}_m\|$ enters the switching zone to reduce the observer error. Notably, T_s should be selected in a way to prevent repetitive switching. The conditions for choosing the switching zone and the switching time are defined in [11].

The estimation results of the designed observers based on switching-gain concept is presented in Fig. 5. The initial gain set, $\varepsilon_1 = 0.32$ and $\varepsilon_2 = 0.45$, was switched to $\varepsilon_1 = 0.9$ and $\varepsilon_2 = 0.9$, $T_s = 45$ min after entering the switching zone. As expected, the observers convergence rates were shorter than Case 1 while their errors are less than Case 2. Therefore, in general, the performance of the observer was improved.

V. DISCUSSION

The model used in designing the observer is a modification of the animal model presented in [8] which, according to the best knowledge of the authors, is the only available bi-hormonal IP model for control purposes. The performance of

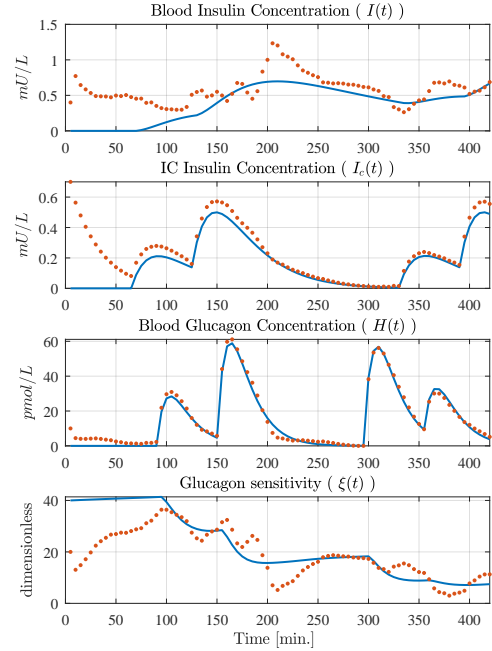


Fig. 4. Case 2: Performance of the designed observer with $\varepsilon_1 = 0.32$ and $\varepsilon_2 = 0.45$. The constant blue lines in this figure show the values of the states derived from the model, while the red dots are the outputs of the observers.

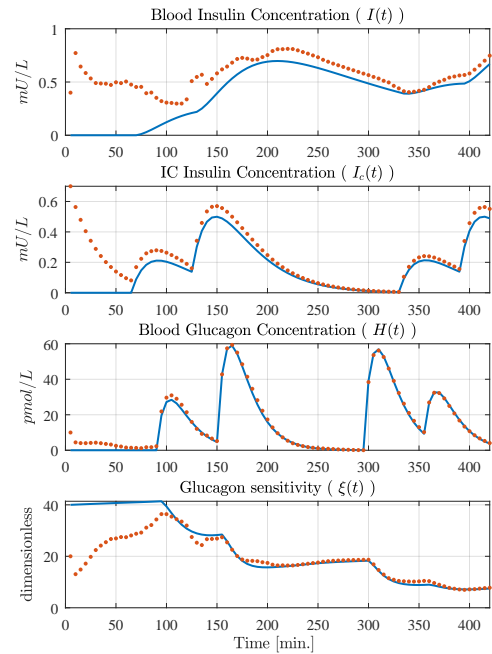


Fig. 5. Performance of the switching gain observer with $\varepsilon_1 = 0.32$ and $\varepsilon_2 = 0.45$ which switches to $\varepsilon_1 = 0.90$ and $\varepsilon_2 = 0.90$ at $T_s = 140$ min. The constant blue lines in this figure show the values of the states derived from the model, while the red dots are the outputs of the observers.

the original model was tested on pigs. Due to the similarity between pigs and human physiology, the model can be used as an alternative for humans. However, the model's performance on T1D patients and consequently the performance of the designed observer can also be evaluated using human trials with realistic inputs.

In evaluating the performance of the observers, noise and the disturbances in measurements, as well as the 15% parameter identification error, were taken into account. The glucose appearance rate, on the other hand, was assumed to be known. However, as shown in (31) and (28), disturbance in R which can be due to an unannounced meal, is calculated in the observer error bound. Therefore, the observer will remain stable for adequately limited disturbances due to unannounced food intake.

VI. CONCLUSIONS

Estimating non-measurable states in the bi-hormonal-glucose model provides a better understanding of the system status and improves the decision-making of a controller in AP. In this regard, two nonlinear high-gain observers were designed separately for the insulin and glucagon phases. It was mathematically shown that the observers are robust against measurement noises, model uncertainties, and disturbances and the closed-loop stability was proven for any asymptotically stable control approaches. Moreover, the simulation results, also confirmed the convergence of the observer to a bounded error. In addition, the performance of the observer was improved by utilizing the switching-gain approach. As a result, the intended observers can be employed in APs to help model-based controllers make better decisions. For example, whenever glucagon sensitivity is estimated to be low, the controller should be extra cautious about the dosage of insulin in order to prevent hypoglycemia.

ACKNOWLEDGMENT

This research is funded by the Research Council of Norway (project no. 248872) and is part of the Centre for Digital Life Norway. We would like to thank Professor Jan Tommy Gravdahl for help in designing the observer and in the discussions.

REFERENCES

- [1] A. Katsarou, S. Gudbjörnsdóttir, A. Rawshani, D. Dabelea, E. Bonifacio, B. J. Anderson, L. M. Jacobsen, D. A. Schatz, and Å. Lernmark, "Type 1 diabetes mellitus," *Nature reviews Disease primers*, vol. 3, no. 1, pp. 1–17, 2017.
- [2] P. Herrero, J. Bondia, N. Oliver, and P. Georgiou, "A coordinated control strategy for insulin and glucagon delivery in type 1 diabetes," *Computer methods in biomechanics and biomedical engineering*, vol. 20, no. 13, pp. 1474–1482, 2017.
- [3] C. Cobelli, E. Renard, and B. Kovatchev, "Artificial pancreas: past, present, future," *Diabetes*, vol. 60, no. 11, pp. 2672–2682, 2011.
- [4] S. J. Moon, I. Jung, and C.-Y. Park, "Current advances of artificial pancreas systems: A comprehensive review of the clinical evidence," *Diabetes & Metabolism Journal*, vol. 45, no. 6, pp. 813–839, 2021.
- [5] C. Toffanin, L. Magni, and C. Cobelli, "Artificial pancreas: In silico study shows no need of meal announcement and improved time in range of glucose with intraperitoneal vs. subcutaneous insulin delivery," *IEEE Transactions on Medical Robotics and Bionics*, vol. 3, no. 2, pp. 306–314, 2021.

- [6] C. D. Man, F. Micheletto, D. Lv, M. Breton, B. Kovatchev, and C. Cobelli, "The uva/padova type 1 diabetes simulator: new features," *Journal of diabetes science and technology*, vol. 8, no. 1, pp. 26–34, 2014.
- [7] B. W. Bequette, "Algorithms for a closed-loop artificial pancreas: the case for model predictive control," *Journal of diabetes science and technology*, vol. 7, no. 6, pp. 1632–1643, 2013.
- [8] C. Lopez-Zazueta, A. L. Fougner *et al.*, "Low-order nonlinear animal model of glucose dynamics for a bihormonal intraperitoneal artificial pancreas," *IEEE Transactions on Biomedical Engineering*, 2021.
- [9] V. Claassen, "Intraperitoneal drug administration," *Neglected factors in pharmacology and neuroscience research*, vol. 12, pp. 46–58, 1994.
- [10] H. K. Khalil and L. Praly, "High-gain observers in nonlinear feedback control," *International Journal of Robust and Nonlinear Control*, vol. 24, no. 6, pp. 993–1015, 2014.
- [11] J. H. Ahrens and H. K. Khalil, "High-gain observers in the presence of measurement noise: A switched-gain approach," *Automatica*, vol. 45, no. 4, pp. 936–943, 2009.
- [12] K. D. Benam, H. Talebi, and M. A. Khosravi, "Full order high gain observer design for image-guided robotic flexible needle steering," in *2019 27th Iranian Conference on Electrical Engineering (ICEE)*. IEEE, 2019, pp. 1151–1156.